



Combined effects of Darcy and Viscous Dissipation on Steady Natural Convection flow in a Vertical Tube partially filled with Porous Material with asymmetric thermal boundary conditions

Deborah Abiola Daramola¹, Babatunde Aina², Jeremiah Jerry Gambo²

¹Department of Mathematics, Air Force Institute of Technology, Kaduna, Nigeria

²Department of Mathematics, Federal University, Gashua, Yobe, Nigeria

Corresponding author's Email: debola32000@yahoo.com

Received on: April, 2024

Revised and Accepted on: May, 2024

Published on: July, 2024

ABSTRACT

This paper examines the impact of Darcy and Viscous dissipation on the hydrodynamic and thermal behavior of steady natural convection in a fully developed incompressible fluid flowing through a vertical composite tube with asymmetric thermal boundary conditions. The fluid motion in the tube is driven by a temperature gradient resulting from heat applied to the tube wall. The study employs the Brinkman-Darcy extended model to simulate fluid flow for both water and air working fluids. The homotopy perturbation method was chosen to solve the temperature and velocity equations for both clear and porous fluids. This method was selected because it systematically decouples the system and overcomes the limitations associated with small parameters in the commonly used perturbation method. Additionally, the homotopy perturbation approach highlights the interactions between parameters that are hidden in numerical methods. An increase in the Brinkman number enhances both the temperature and velocity profiles of the working fluids. Similarly, increasing the thickness of the porous material can boost the fluid's velocity in the composite vertical tube. A rise in the material's porosity also leads to an increase in fluid velocity.

Keywords: Natural convection, Viscous dissipation, Porous medium, Homotopy Perturbation Method (HPM).

1.0 INTRODUCTION

Fluid flow has garnered significant attention due to its wide-ranging applications in Science, Engineering, and industrial technologies, including gas drainage, cooling of electrical appliances, geothermal energy, plasma physics, gas turbines, fossil fuel combustion, and food processing industries, among others. The critical role of fluid flow in composite tubes within science and engineering has made it a focal point of scholarly research. Viscous dissipation refers to the internal heat generation resulting from viscous forces in molecular fluid-particle interactions. The mechanical energy released through this process significantly influences the thermal buoyancy and behavior of a moving fluid. Since fluid-particle interactions affect both fluid flow and temperature, viscous dissipation is crucial in many lubrication systems.

One of the earliest works on viscous dissipation was by Gebhart (1962), who used the perturbation method to study its effect on natural convection flow under both isothermal and uniform flux conditions. Pantokratoras (2005) examined the impact of viscous dissipation on natural convection flow along a vertically heated plate, concluding that it enhances upward flow by increasing the buoyant force. In another study, Jha and Ajibade (2012) investigated unsteady natural convection flow influenced by viscous dissipation, finding that its effect on temperature is more pronounced when the fluid has a

relatively low Prandtl number. Fully developed natural convection flow in a vertical parallel plates microchannel in the presence of viscous dissipation is theoretically examined by Jha and Aina (2019). They demonstrated that an increase in the value of rarefaction parameter decreases the effect of viscous dissipation on the Nusselt number. Ajibade and Umar (2019) theoretically investigated the influence of viscous dissipation and wall conduction on steady mixed convection Couette flow of heat generating and absorbing fluid. Magnetohydrodynamic natural convection flow in a vertical parallel plate microchannel in the presence of viscous and joulean dissipation is theoretically examined by Aina et al. (2021). Ajibade *et al.* (2021) used the homotopy perturbation method to study the effect of viscous dissipation on steady MHD natural convection Couette flow, showing that viscous dissipation significantly influences the hydrodynamic and thermodynamic distributions of the fluids. Ajibade *et al.* (2021) carried out an analytical study on effects of viscous dissipation and suction on steady MHD natural convection Couette flow of heat generating or absorbing fluid. Impact of viscous dissipation and Coriolis effects in heat and mass transfer analysis of the 3D non-Newtonian fluid flow was examined by Alhandi et al. (2022). The work of Aina and Daramola (2022) deals with a theoretical investigation of the effect of viscous dissipation on buoyancy induced flow in a vertical permeable microchannel in the presence of velocity slip



and temperature jump. Ajibade *et al.* (2022) examined the combined effects of viscous and Darcy dissipation in mixed convection flow in a composite vertical channel partially filled with porous material. They found that the Brinkman number enhances the temperature and velocity profiles, and that increasing the porosity of the porous material can be used to control the pressure gradient driving the flow in the composite channel. In a recent study, Lilian *et al.* (2023) investigated the effect of viscous dissipation on temperature distribution of blood plasma in the presence of a magnetic field.

Rodríguez-Núñez *et al.* (2019) found that lateral heating of a vertical cylindrical tube induces dynamic changes in the convective motion of an aqueous solution during the 600-second heating process. The convective flow of air establishes a circulating convection pattern within 5 seconds, which persists for the remainder of the process. In contrast, the aqueous solution within the silica porous medium exhibits slow motion with no significant changes throughout the heating period. They conducted a numerical study on the conjugate unsteady natural heat convection of air over a non-Newtonian polymer water solution, characterized by a power-law model, within a sealed vertical thick-walled cylindrical enclosure partially filled with a porous medium. Also, Charreh and Saleem (2023) investigated fluid flow phenomena, general heat transfer, and entropy generation in transient natural convection within a square cavity filled with a saturated non-Darcy porous medium, considering dissipation effects and thermal radiation. Their findings revealed that Forchheimer resistance increases the flow rate while reducing heat transfer and entropy production. Hussain and Zeeshan (2022) investigated entropy generation in the natural convection of Casson fluid within a porous, partially heated square enclosure, considering the effects of a horizontal magnetic field, cavity inclusion, and viscous dissipation. They found that at small values of the Eckert number $Ec = 10^{-6}$, there is minimal variation in the average heat transfer rate since viscous dissipation has little impact on the velocity profile within the cavity. Consequently, increasing the viscous dissipation effect does not significantly alter the entropy generation due to fluid friction. However, the increase in viscous dissipation leads to greater internal heat generation, decreasing the average Nusselt number. Jagadha and Amrutha (2019) investigated the laminar viscous incompressible nanofluid flow involving mixed convection and mass transfer around an isothermal vertical flat plate embedded in a Darcy porous medium, considering the effects of a magnetic field and the viscous effective thermal conductivity of the porous medium, their study revealed that as the Eckert number (Ec) increases, the fluid velocity also increases, while the Nusselt number decreases.

The importance of convective flow in porous media has grown due to its expanding practical applications in areas such as the petroleum industry, electronic cooling, porous solids drying, thermal insulation, packed-bed catalytic reactors, and geothermal reservoirs. Ajibade and Umar (2016) investigated an unsteady MHD natural convection flow in a vertical channel filled with porous materials, concluding that an increase in permeability parameters leads to an increase in velocity profiles. The effects of viscous and Darcy dissipation on mixed convection in a vertical channel filled with a porous substance, concluding that the Darcy parameter drag term suppresses fluid flow. Mahdy *et al.* (2021) investigated convective flow of a micropolar hybrid nanofluid through a vertical radiating permeable plate in a saturated porous medium, observing that increases in micropolarity and nanoparticle volume fraction enhance the skin friction coefficient and Nusselt number.

Barnoon *et al.* (2019) studied non-Newtonian nanofluid flow and heat transfer in a permeable enclosure with two cylinders embedded in a cavity, with and without thermal radiation. They found that heat transfer could either increase or decrease depending on the size of the cylinder. According to Venkatadri *et al.* (2023), free convective flows in a right-angled trapezoidal cavity saturated with a porous bed and filled with Cu-water nanofluid material revealed that as the Darcy number (Da) increases, the flow rate spreads throughout the porous area, influenced by the harmonic motion of the fluid. According to Amoli *et al.* (2022), an experimental and numerical analysis of laminar forced convection flow in a horizontal pipe partially filled with a porous medium under a constant heat flux. Their findings showed that an eccentric placement of the porous material reduces both the heat transfer coefficient and the pressure drop. However, the reduction in the heat transfer coefficient is less significant when the thickness of the porous medium is smaller. Hamza *et al.* (2022) examined the impact of magnetohydrodynamics on the unsteady fluid flow of an exothermic reaction within a vertical channel filled with porous media. Their study found that an increase in permeability led to enhanced fluid flow, resulting in a rise in fluid velocity. Additionally, as the Biot number increases, both the surface and internal temperatures of the channel also increase. Girish and Sankar (2020) observed that the baffle position, Darcy number, modified Grashof number, and Brinkman number significantly influence the flow fields, while the thermal fields are notably affected by the Brinkman number, Darcy number, and baffle position. They conducted both analytical and numerical investigations of fully developed mixed convection in a vertical double-passage annulus filled with porous media. Their findings revealed

that the magnitude of velocity decreases as the Darcy number decreases.

To date, a lot of work has been conducted on the effect of viscous dissipation. Nevertheless, to the best of the author's knowledge, there is no investigation on impact of Darcy and Viscous dissipation on the hydrodynamic and thermal behavior of steady natural convection in a fully developed incompressible fluid flowing through a vertical composite tube with asymmetric thermal boundary conditions.

2.0 MATERIALS AND MATHEMATICAL ANALYSIS

Consider a steady flow of a viscous incompressible fluid in an infinite vertical tube, as depicted in Figure 1. The region near $r' = 0$ is occupied by clear fluid, while the section near $r' = a$ is filled with a fully saturated porous medium. The clear fluid and the porous region are separated by an interface at $r' = d'$. The flow direction is aligned with the vertical axis, and the r' -axis is oriented radially. The fluid motion is driven by natural convection, resulting from density changes due to temperature variations.

The energy equations account for viscous dissipation in the clear fluid region, while both Darcy and viscous dissipation are considered in the porous medium section. The temperatures of the porous medium and the clear fluid are assumed to be equivalent, satisfying the local thermal equilibrium (LTE) condition. The governing equations are presented below in their dimensional form, using the standard Boussinesq approximation:

$$\mu \left(\frac{d^2 u'_f}{dr'^2} + \frac{1}{r'} \frac{du'_f}{dr'} \right) + g\rho\beta(T'_f - T_0) = 0, \tag{1}$$

$$\mu_{eff} \left(\frac{d^2 u'_p}{dr'^2} + \frac{1}{r'} \frac{du'_p}{dr'} \right) - \frac{\mu u'_p}{K} + g\rho\beta(T'_p - T_0) = 0, \tag{2}$$

$$k \left(\frac{d^2 T'_f}{dr'^2} + \frac{1}{r'} \frac{dT'_f}{dr'} \right) + \mu \left(\frac{du'_f}{dr'} \right)^2 = 0, \tag{3}$$

$$k \left(\frac{d^2 T'_p}{dr'^2} + \frac{1}{r'} \frac{dT'_p}{dr'} \right) + \left(\mu_{eff} \left(\frac{du'_p}{dr'} \right)^2 + \frac{\mu u'^2}{K} \right) = 0 \tag{4}$$

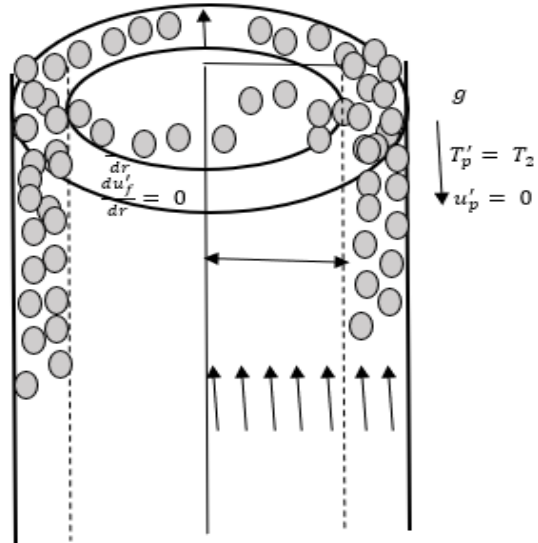


Figure 1. Schematic Diagram

The boundary and interfacial conditions in dimensional form are;

$$\begin{aligned} \frac{du'_f}{dr'} = 0, & \quad \frac{dT'_f}{dr'} = 0, \\ 0, & \quad r' = 0 \\ u'_p = 0, & \quad T'_p = T_2, \\ T_2, & \quad r' = a \end{aligned} \tag{5}$$

$$\begin{aligned} r' = d' \{ u'_f = u'_p, & \quad T'_f = T'_p \\ \mu_{eff} \frac{du'_p}{dr'} - \mu \frac{\alpha u'_f}{dr'} = \mu \frac{\alpha u'_p}{\sqrt{K}}, & \quad \frac{dT'_f}{dr'} = \frac{dT'_p}{dr'} \end{aligned} \tag{6}$$

The governing equations (1) – (4), along with the boundary and interfacial conditions (5) and (6), are expressed in dimensionless form as follows:

$$\frac{d^2 u_f}{dr^2} + \frac{1}{r} \frac{du_f}{dr} + \theta_f = 0, \tag{7}$$

$$\gamma \left(\frac{d^2 u_p}{dr^2} + \frac{1}{r} \frac{du_p}{dr} \right) - \frac{u_p}{Da} + \theta_p = 0, \tag{8}$$

$$\frac{d^2 \theta_f}{dr^2} + \frac{1}{r} \frac{d\theta_f}{dr} + Br \left(\frac{du_f}{dr} \right)^2 = 0, \tag{9}$$

$$\frac{d^2 \theta_p}{dr^2} + \frac{1}{r} \frac{d\theta_p}{dr} + Br \left(\left(\gamma \frac{du_p}{dr} \right)^2 + \frac{u_p^2}{Da} \right) = 0 \tag{10}$$

subject to the following dimensionless initial and boundary conditions:

$$\begin{aligned} \frac{du_f}{dr} = 0, & \quad \frac{d\theta_f}{dr} = 0, & \text{at } r = 0 \\ u_p = 0, & \quad \theta_p = 0.5, & \text{at } r = 1 \end{aligned} \tag{11}$$

$$\begin{aligned} r = d \{ u_f = u_p, & \quad \theta_f = \theta_p \\ \frac{\alpha}{\sqrt{Da}} u_f, & \quad \frac{d\theta_f}{dr} = \frac{d\theta_p}{dr} \end{aligned} \tag{12}$$



Defining a reference average temperature

$$T_0 = \frac{T_1 + T_2}{2}$$

the dimensionless equation (7) - (10) associated with the conditions (11) and (12) contain the following dimensionless quantities:

$$\begin{aligned} \gamma &= \frac{\mu_{eff}}{\mu}, & u_p &= \frac{u'_p}{u_0}, & u_f &= \frac{u'_f}{u_0}, \\ \vartheta &= \frac{\mu}{\rho}, & \theta_p &= \frac{T'_p - T_0}{T_2 - T_1}, \\ \theta_f &= \frac{T'_f - T_0}{T_2 - T_1}, & z &= \frac{d'}{a}, & Da &= \frac{r^2}{K}, \\ r &= \frac{r'}{a} \end{aligned} \tag{13}$$

3.0 METHOD OF SOLUTION/ METHODOLOGY

Considering the following non-linear differential equation:

$$A(u) - f(r) = 0, \quad r \in \Omega \tag{14}$$

subject to the boundary conditions

$$B\left(u, \frac{\partial u}{\partial n}\right) = 0, \quad r \in \Gamma \tag{15}$$

where A represents the general differential operator, B is the boundary operator, $f(r)$ is a known analytic function, and Γ denotes the domain boundary. The non-linear differential equation can be expressed as follows. The operator A can be decomposed into two components: L , which is the linear part, and N , which is the non-linear part, as follows:

$$L(u) + N(u) - f(r) = 0, \tag{16}$$

Convex Homotopy is constructed from the non-linear differential equation and its boundary condition as:

$$v(r, \rho): \Omega \times [0, 1] \rightarrow R \text{ which satisfies}$$

Now, the solution of the momentum and energy equation both in the clear and porous regions of the fluid as $\rho \rightarrow 1$ are:

$$u_f = k_3 + k_8 + k_1 r^2 \tag{28}$$

$$u_p = k_2 r^2 + k_4 \ln \ln(r) - k_2 + k_5 r^4 + k_6 r^2 + k_7 r^2 \ln \ln(r) + k_9 \ln \ln(r) + k_{10} \tag{29}$$

$$\theta_f = 0.5 + k_{29} + k_{19} r^4 \tag{30}$$

$$\theta_p = 0.5 + k_{20} r^6 + k_{21} r^4 + k_{22} r^4 \ln \ln(r) + k_{23} r^2 + k_{24} r^2 \ln \ln(r) + k_{25} \ln \ln(r)^2 r^2 + k_{26} \ln \ln(r)^2 + k_{30} \ln \ln(r) + k_{31} \tag{31}$$

Due to the complexity of the other terms in the equation, they will not be included here. The heat transfer in the tube is characterized by the Nusselt number, which can be calculated in dimensionless form as follows:

$$Nu_1 = \left. \frac{d\theta_p}{dr} \right|_{r=1} \tag{32}$$

$$H(v, \rho) = (1 - \rho)[L(u) - L(u_0)] + \rho[A(u) - f(r)] = 0, \tag{17}$$

or

$$H(v, \rho) = L(u) - L(u_0) + \rho L(u_0) + \rho[N(u) - f(r)] = 0, \tag{18}$$

where $\rho \in [0, 1]$ is an embedding parameter, u_0 is the initial approximation of equation (14) that satisfies the general boundary condition. Consequently, from equations (17) and (18), we obtain:

$$H(v, 0) = L(v) - L(u_0) = 0. \tag{19}$$

$$H(v, 1) = A(v) - f(r) = 0. \tag{20}$$

The nonlinear differential equation's solution is now written as:

$$v = v_0 + \rho v_1 + \rho^2 v_2 + \rho^3 v_3 + \dots \tag{21}$$

Setting $\rho = 1$, the approximate solution is written as

$$v = v = v_0 + v_1 + v_2 + v_3 + \dots \tag{22}$$

For the current problem, the convex homotopy of the momentum and energy equations is constructed as follows:

$$H(u, \rho) = (1 - \rho) \left[\frac{d^2 u_f}{dr^2} + \frac{1}{r} \frac{du_f}{dr} \right] \tag{23}$$

Setting u_f, u_p, θ_f and θ_p as infinite series such that

$$u_f = u_{f_0} + \rho u_{f_1} + \rho^2 u_{f_2} + \rho^3 u_{f_3} + \dots \tag{24}$$

$$u_p = u_{p_0} + \rho u_{p_1} + \rho^2 u_{p_2} + \rho^3 u_{p_3} + \dots \tag{25}$$

$$\theta_f = \theta_{f_0} + \rho \theta_{f_1} + \rho^2 \theta_{f_2} + \rho^3 \theta_{f_3} + \dots \tag{26}$$

$$\theta_p = \theta_{p_0} + \rho \theta_{p_1} + \rho^2 \theta_{p_2} + \rho^3 \theta_{p_3} + \dots \tag{27}$$

4.0 RESULTS AND DISCUSSIONS

This section examines the impact of various flow parameters on the thermodynamics and hydrodynamics within the composite tube. The results, represented

through line graphs in Figures 2–9, were derived from the approximation solutions. For water and air as the working fluids at 1 atm pressure, the following values are used: for water: $\mu = 1.002 \times 10^{-3} \text{ kg/ms}$ at 20°C , $\beta = 2.09 \times 10^{-4} \text{ }^\circ\text{C}^{-1}$, $g = 9.8 \text{ m}^2/\text{s}$, $k = 0.5861 \text{ W/mk}$, $\nu = 1.003 \times 10^{-6} \text{ m}^2/\text{s}$, $u_0 = 5.0 \text{ m/s}$ and $H = 1.0 \text{ m}$ and for air at 1 atm pressure we have $\mu = 1.806 \times 10^{-5} \text{ kg/ms}$ at 20°C , $\beta = \frac{1}{293} \text{ }^\circ\text{C}^{-1}$, $g = 9.8 \text{ m}^2/\text{s}$, $k = 0.024 \text{ W/mk}$, $\nu = 1.5 \times 10^{-5} \text{ m}^2/\text{s}$, $u_0 = 5.0 \text{ m/s}$ and $H = 1.0 \text{ m}$ are taken into account.

Table 1: Computed Values of Brinkman number

$Br = \frac{\mu g^2 \beta^2 H^4 (T_2 - T_1)}{k}$		
$T_2 - T_1$	Air	Water
20 °C	100.7436	93.0180
40 °C	201.4872	186.0361
60 °C	302.2309	279.0541

Description: shows several computed values Brinkman number, Br for both air and water at different temperatures.

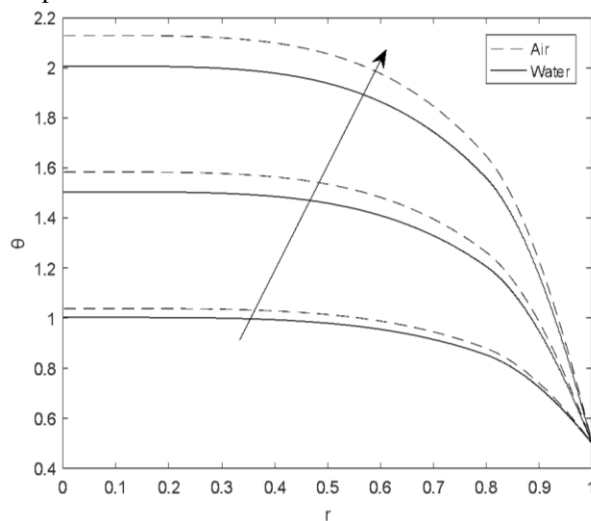


Figure 2: Effects of Br on Temperature profile

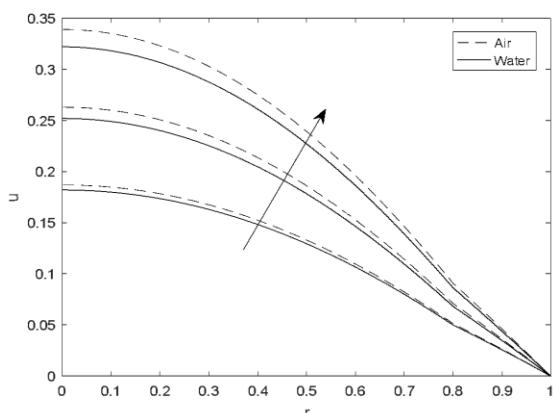


Figure 3: Effects of Br on Velocity profile

Figures 2 and 3 illustrate the effects of the Brinkman number on the temperature and velocity profiles, with the Darcy number fixed at ($Da = 0.1$), the thickness of the porous region ($d = 0.8$), the adjustable coefficient ($\alpha = 0.5$) and viscosity ratio ($\gamma = 1.0$). Both fluid velocity and temperature profiles for air and water increase with a rise in the Brinkman number. As the Brinkman number increases, viscous dissipation enhances the thermal energy generated within the fluid in the channel. This results in higher fluid velocities in both the porous region and the free flow region, which are associated with increased Brinkman number values, leading to greater internal heat production. Consequently, the fluid temperature rises due to viscous dissipation, which in turn increases buoyancy force and fluid velocity. Notably, the impact of the Brinkman number is more pronounced for air compared to water.

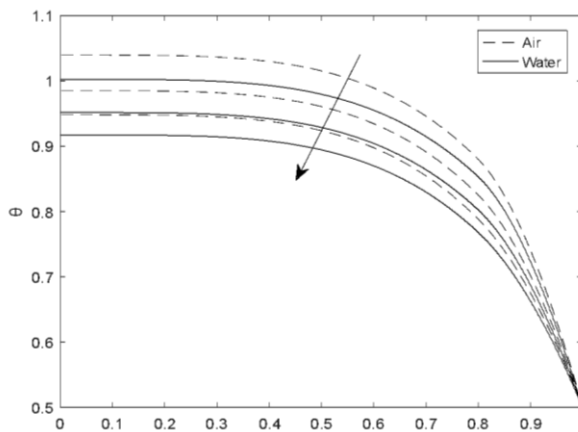


Figure 4: Effects of Da on Temperature profile

Figures 4 and 5 illustrate the effects of the Darcy number on the temperature and velocity profiles, with the Brinkman number ($Air = 100, Water = 93$), the thickness of the porous region set at ($d = 0.8$), the adjustable coefficient ($\alpha = 0.5$) and viscosity ratio ($\gamma = 1.0$). As the Darcy number increases, the temperature profile decreases while the velocity profile increases. When the Darcy number is high, the porous medium behaves more like a transparent fluid region, whereas a low Darcy number makes the porous region act like a solid material with significant resistance. Figure 4 supports this observation, as a higher Darcy number reduces the resistance of the porous material, thereby decreasing fluid-particle collisions and lowering heat generation due to Darcy's dissipation. Consequently, the temperature decreases. Conversely, as the Darcy number (Da) increases, the permeability of the porous material rises, reducing its retardation effect and facilitating

greater fluid movement within the composite tube, leading to an increase in velocity.

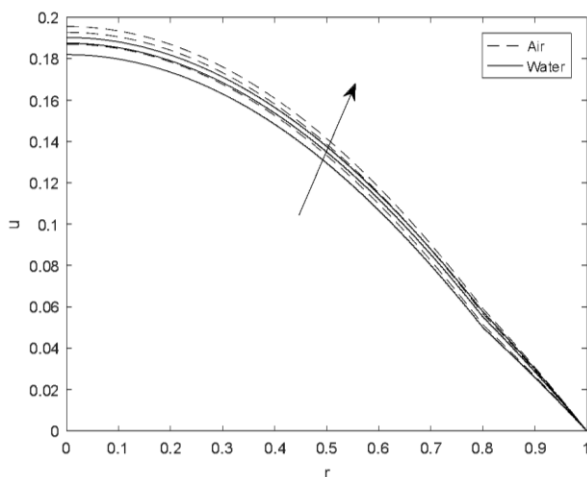


Figure 5: Effects of Da on Velocity profile

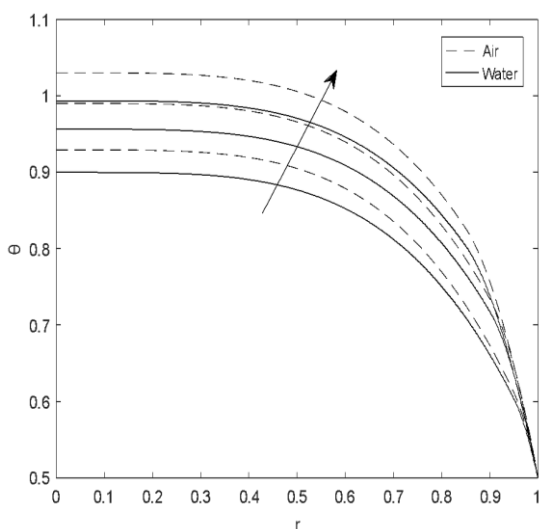


Figure 6: Effects of d on Temperature profile

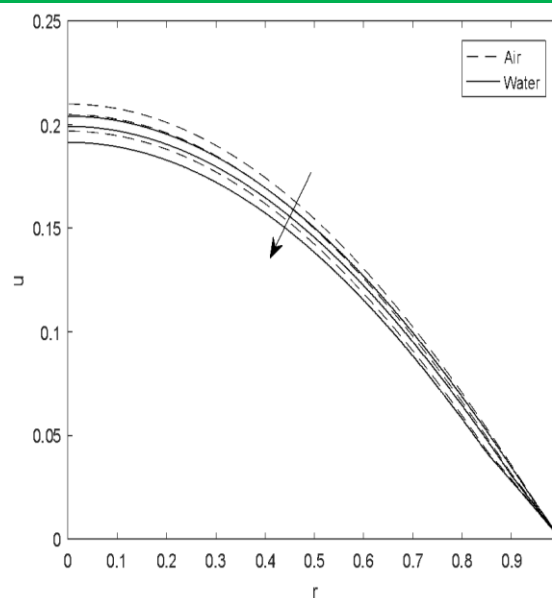


Figure 7: Effects of d on Velocity profile

Figures 6 and 7 illustrate the relationship between temperature and velocity as functions of the thickness of the porous zone. An increase in the thickness of the porous layer leads to a proportional rise in temperature. This effect is attributed to the addition of the Darcy dissipation term to the viscous dissipation term, which results in increased heat generation. Conversely, as the thickness of the porous region increases, the velocity within the porous zone decreases. This decrease is due to the increasing retarding effect of the thicker porous medium. Table 2 shows the rate of heat transfer in the tube with fixed values of $\gamma = 1.0, \alpha = 0.5$. An increase in the thickness of the porous material results in a decrease in the rate of heat transfer within the tube. This reduction occurs because a thicker porous material diminishes the temperature difference between the tube wall and the fluid, thereby lowering the heat transfer rate. Additionally, the rate of heat transfer is observed to increase with higher Brinkman numbers. Notably, the rate of heat transfer is higher for air compared to water.

Table 2: Rate of Heat Transfer

d	$Nu_1(Air)$			$Nu_1(Water)$		
	Br	$Da = 0.1$	$Da = 0.2$	Br	$Da = 0.1$	$Da = 0.2$
0.05	100	3.1012	2.0946	93	2.8841	1.9479
	201	6.2334	4.2101	186	5.7682	3.8959
	302	9.3565	6.3256	279	8.6523	5.8438
0.20	100	2.8584	2.3866	93	2.6583	2.2195
	201	5.7454	4.7970	186	5.3166	4.4390
	302	8.6323	7.2075	279	7.9749	6.6586

5.0 CONCLUSION

The current study investigated steady natural convection flow in a vertical composite tube partially filled with



porous material, considering the effects of Darcy and viscous dissipation. The governing equations were solved using the Homotopy Perturbation Method (HPM). The main findings are summarized as follows:

- i. An increase in the Brinkman number results in higher temperatures and velocities for both fluids.
- ii. Increasing the thickness of the porous material enhances the fluid velocity within the composite vertical tube.
- iii. An increase in the material's porosity also leads to a higher fluid velocity.

REFERENCES

- B. Gebhart, 'Effects of viscous dissipation in natural convection', *J Fluid Mech*, vol. 14, no. 2, pp. 225–232, 1962, doi: 10.1017/S0022112062001196.
- A. Pantokratoras, 'Effect of viscous dissipation in natural convection along a heated vertical plate', *Appl Math Model*, vol. 29, no. 6, pp. 553–564, Jun. 2005, doi: 10.1016/j.apm.2004.10.007.
- B. K. Jha and A. O. Ajibade, 'Effect of viscous dissipation on natural convection flow between vertical parallel plates with time-periodic boundary conditions', *Commun Nonlinear Sci Numer Simul*, vol. 17, no. 4, pp. 1576–1587, 2012, doi: 10.1016/j.cnsns.2011.09.020.
- A. O. Ajibade, A. M. Umar, and T. M. Kabir, 'An analytical study on effects of viscous dissipation and suction/injection on a steady MHD natural convection Couette flow of heat generating/absorbing fluid', *Advances in Mechanical Engineering*, vol. 13, No. 5, 2021, doi: 10.1177/16878140211015862.
- A.O.Ajibade, B. K. Jha, and J.J.Gambo, 'Combined effect of viscous and Darcy dissipation in mixed convection flow in a composite vertical channel partially filled with porous material ; Analytical method', *International Communication in Heat and Mass Transfer*, vol. 136, doi.org/10.1016/j.icheatmasstransfer, 2022.106197.
- M. M. Lilian, J. Kerongo, V. Bulinda, 'Effects of viscous dissipation on temperature distribution of blood plasma in presence of a magnetic field', *Applied Mathematics*, Vol. 14, No. 9, Sept. 22, 2023
- K. A. M. Alhandi, A. Ullah, I. Fatima, R. Khan, R. Sahanl, M. Khan, S. Khan and F. Ali, 'Impact of viscous dissipation and coriolis effect in heat and mass transfer analysis of the 3D non-Newtonian fluid flow', *Case Studies in Thermal Engineering*, 37, Article ID: 102289, 2022
- A. O. Ajibade, and A. M. Umar, 'Effects of viscous and wall conduction on steady mixed convection couette flow of heat generating and absorbing fluid', vol. 24, no, 4, pp. 12-45, 2021
- B. Aina, S. Isa and D. Daramola, 'Properties of Viscous and Joulean Dissipation on fully Developed natural convection in a vertical microchannel in existence of Lorente forces, FuLafia Journal of Science and Technology (FJST), 7(1), pp.42-49, 2021
- B. Aina, and D. Daramola, 'Effects of Viscous Dissipation and Suction-Injection Combination (SIC) on Free Convection flow in a vertical Permeable Micro-Channel, AFIT Journal of Science and Engineering Research, 2 (2), pp. 76-83, 2022
- A. O. Ajibade and A. M. Umar, 'Steady natural convection Couette flow with wall conduction and thermal boundary condition of third kind', *ZAMM Zeitschrift fur Angewandte Mathematik und Mechanik*, vol. 100, no. 8, pp. 1–18, 2020, doi: 10.1002/zamm.201900095.
- A. Mahdy, E.R. El-Zahar, A. M. Rashad, W. Saad and H. S. Al- Juaydi, 'The Magneto- Natural Convection flow of a micropolar hybrid nanofluid over a vertical plate saturated in a porous medium' *Fluids* 2021,6,202 doi.org/10.3390/fluid 6060202.
- P. Barnoon, D. Toghraie, R. B. Dehkordi and M.Afrand, ' Two phase natural convection and thermal [34] radiation of non-Newtonian nanofluid in a porous cavity considering inclined cavity and size of inside cylinders' *Internal Communication in Heat and Mass transfer* 108(2019), doi.org.10/1016/j.icheatmasstransfer 2019.104285
- K. Venkatadri, F. O. Syed, A. Beg, O.Ramesh, ' Natural convection of nanofluid flow in a porous medium in a right-angled trapezoidal enclosure; a Tiwari and Das nanofluid model' *Journal of Taibah University for Science* , 2023, doi.10.1080/16583655.2023.226324
- A. O. Ajibade, J. J.Gambo, and B. K. Jha, ' Effect of Darcy and Viscous Dissipation on Natural convection flow in a vertical tube partially filled with porous material under convective boundary condition. *Int. J. Appl. Comput. Math*(2024)1084. <https://doi.org/10.1007/s40819-023-01623-2>
- A. O. Ajibade, J. J.Gambo, and B. K. Jha, ' Effect of Darcy and Viscous Dissipation on fully developed Natural convection flow in a composite channel partially filled with porous material; homotopy perturbation method (HPM) *ZAMM J. Appl. Math. Mech*(2023)<https://doi.org/10.1002/zamm.202100583>
- K. Rodríguez-Núñez, E. Tabilo and N. O. Moraga (2019). Conjugate unsteady natural heat convection of air and non-Newtonian fluid in thick walled cylindrical enclosure partially filled with a porous media. *International Communications in Heat and Mass Transfer*, 108, 104304.
- D. Charreh, and M. Saleem (2023). Entropy generation and natural convection analyses in a non-Darcy porous



square cavity with thermal radiation and viscous dissipation. *Results in Physics*, 52, 106874.

B. S. Amoli, S. S. M. Ajarostaghi, M. Saffar-Avval, R. H. Abardeh, and N. Akkurt (2022). Experimental and numerical analysis of forced convection in a horizontal tube partially filled with a porous medium under local thermal equilibrium conditions. *Water*, 14(23), 3832.

S. Hussain and M. Zeeshan (2022). Irreversibility analysis for the natural convection of Casson fluid in an inclined porous cavity under the effects of magnetic field and viscous dissipation. *International Journal of Thermal Sciences*, 179, 107699.

S. Jagadha and P. Amrutha (2019). MHD boundary layer flow of Darcy-Forchheimer mixed convection in a nanofluid saturated porous media with viscous dissipation. *Applications and Applied Mathematics: An International Journal (AAM)*, 14(4), 10.

M. M. Hamza, A. Shuaibu and A. S. Kamba (2022). Unsteady MHD free convection flow of an exothermic fluid in a convectively heated vertical channel filled with porous medium. *Scientific reports*, 12(1), 11989.

N. Girish and M. Sankar (2020). Fully developed mixed convection in vertical double passage porous annuli. In *Journal of Physics: Conference Series* (Vol. 1597, No. 1, p. 012050). IOP Publishing.

Nomenclature

z	Non-dimensional thickness of porous region	
z'	Dimensional thickness of porous region	
Da	Darcy number	
Br	Brinkman number	
y'	Dimensional coordinate	
y	Non-dimensional horizontal coordinate	
u'	Fluid velocity in dimensional form	$[ms^{-1}]$
u	Fluid velocity in dimensionless form	
T_0	Reference temperature	$[K]$
T_1	Temperature at the wall $y = 0$	$[K]$
T_2	Temperature at the wall $y = h$	$[K]$
g	Acceleration due to gravity	$[ms^{-2}]$

Greek symbols

a	Adjustable coefficient in the stress jump condition	
β	Coefficient of thermal expansion	$[K^{-1}]$
γ	Ratio of viscosity	
μ_{eff}	Effective kinematic viscosity of the porous medium	$[m^2s^{-1}]$
μ	Kinematic viscosity of the fluid	$[m^2s^{-1}]$
ρ	Density	$[Kgm^{-3}]$

Subscripts

f	Clear fluid region
i	Interface between clear fluid and porous region
p	Porous region
W	Water
A	Air